

PRECISE TIMING OF THE X-RAY PULSAR 1E 1207.4–5209: A STEADY NEUTRON STAR WEAKLY MAGNETIZED AT BIRTH

E. V. GOTTHELF & J. P. HALPERN

Columbia Astrophysics Laboratory, Columbia University, New York, NY 10027

Submitted to the Astrophysical Journal Letters, April 17 2007

ABSTRACT

We analyze all X-ray timing data on 1E 1207.4–5209 in supernova remnant PKS 1209–51/52 gathered in 2000–2005, and find a highly stable rotation with $P = 424.130751(4)$ ms and $\dot{P} = (9.6 \pm 9.4) \times 10^{-17}$ s s⁻¹. This refutes previous claims of large timing irregularities in these data. In the dipole spin-down formalism, the 2σ upper limit on \dot{P} implies an energy loss rate $\dot{E} < 1.5 \times 10^{32}$ ergs s⁻¹, surface magnetic field strength $B_p < 3.5 \times 10^{11}$ G, and characteristic age $\tau_c \equiv P/2\dot{P} > 24$ Myr. This τ_c exceeds the remnant age by 3 orders of magnitude, requiring that the pulsar was born spinning at its present period. The X-ray luminosity of 1E 1207.4–5209, $L_{\text{bol}} \approx 2 \times 10^{33} (d/2 \text{ kpc})^2$ ergs s⁻¹, exceeds its \dot{E} , implying that L_{bol} derives from residual cooling, and perhaps partly from accretion of supernova debris. The upper limit on B_p is small enough to favor the electron cyclotron model for at least one of the prominent absorption lines in its soft X-ray spectrum. This is the second demonstrable case of a pulsar born spinning slowly and with a weak B -field, after PSR J1852+0040 in Kesteven 79.

Subject headings: ISM: individual (PKS 1209–51/52) — pulsars: individual (1E 1207.4–5209, PSR J1852+0040) — stars: neutron — supernova remnants

1. INTRODUCTION

The neutron star 1E 1207.4–5209 in the center of supernova remnant PKS 1209–51/52 is the first discovered (Helfand & Becker 1984) and most intensively studied of the so-called Central Compact Objects (CCOs). These seemingly isolated NSs are defined by their steady flux, predominantly thermal X-ray emission, lack of optical or radio counterparts, and absence of a surrounding pulsar wind nebula (see Pavlov et al. 2004, for a review). 1E 1207.4–5209 acquired special importance when it became the first CCO in which pulsations were detected (Zavlin et al. 2000; Pavlov et al. 2002). It was distinguished again as the first isolated NS to display strong absorption lines in its X-ray spectrum (Sanwal et al. 2002; Mereghetti et al. 2002; Bignami et al. 2003).

More recently, accumulated X-ray observations of 1E 1207.4–5209 were presented as showing large-amplitude changes of both sign in its spin period (Zavlin et al. 2004) that were unlike any other pulsar and difficult to explain. Consequently, the surface dipole magnetic field, which is a key parameter in all proposed mechanisms for the X-ray absorption lines, could not be estimated independently from the spin-down rate, which was indeterminate. In this Letter, we present a definitive study of the spin history of 1E 1207.4–5209 that corrects previous errors in the data and their analysis. We provide reliable spin parameters and discuss their implications for the interpretation of the X-ray spectrum of 1E 1207.4–5209, and for the origin of the class of CCOs more generally.

2. ARCHIVAL X-RAY OBSERVATIONS (2000–2005)

We reanalyzed all timing data on 1E 1207.4–5209 from the archives of the *Newton X-Ray Multi-Mirror Mission* (*XMM-Newton*) and *Chandra* observatories. They span 2000 January to 2005 July. A log of these observations is given in Table 1.

All 11 *XMM-Newton* observations of 1E 1207.4–5209 used the pn detector of the European Photon Imaging Camera (EPIC-pn) in “small window” (SW) mode to achieve 5.7 ms time resolution. Several EPIC-pn data sets had photon timing errors uncorrected in their original processing (Kirsch et al. 2004). We reprocessed all EPIC data using the emchain and epchain scripts under Science Analysis System (SAS) version xmm-sas_20060628_1801-7.0.0, which produces correct photon time assignments. The observations were affected by background to varying degree. To maximize the signal-to-noise ratio in each, we adjusted the source extraction aperture individually. For this soft source, an energy cut of 0.5 – 2.5 keV was found to maximize pulsed power.

We also examined data simultaneously available from the EPIC MOS camera, operated in “full frame” mode. Although not useful for timing purposes (2.7 s readout), the location of the source at the center of the on-axis MOS CCD allows a better background measurement to test for flux variability, an important indicator of accretion, than the EPIC-pn SW mode. The seven observations of 2005 exhibit root-mean-square source flux variability of less than 1% over the 40 day span. Comparing these count rates to the earlier *XMM-Newton* observation of 2001 December, implies a marginally significant flux decrease of $5\% \pm 3\%$ during the 5 year interval.

Four *Chandra* observations suitable for timing measurements of 1E 1207.4–5209 are available. They used the Advanced Camera for Imaging and Spectroscopy (ACIS) in continuous-clocking (CC) mode to provide time resolution of 2.85 ms. Two of the four observations were taken with the LETG transmission grating in place, the zeroth order image being used for timing. This study uses data processed by the latest pipeline software (revision v7.6.8.1), with the exception of 2000 January 6, which is processed with revision v6.5.1. Reduction and analysis used the standard software package CIAO

TABLE 1
LOG OF X-RAY TIMING OBSERVATIONS AND SUMMARY OF RESULTS

Set	Mission	Instr/Mode	ObsID/Seq#	Date (UT)	Span (ks)	Start Epoch (MJD)	Period ^a (ms)	Z_1^2
1	<i>Chandra</i>	ACIS-S/CC	0751/500249	2000 Jan 06	32.5	51549.625	424.13066(48)	51.6
	<i>XMM</i>	EPIC-pn/SW	0113050501	2001 Dec 23	26.8	52266.799	424.13075(36)	113.1
2	<i>Chandra</i>	ACIS-S/CC	2799/500249	2002 Jan 05	30.4	52279.952	424.13062(38)	62.2
				Set 2 combined:	1167.3	52266.799	424.130748(16)	169.6
3	<i>XMM</i>	EPIC-pn/SW	0155960301	2002 Aug 04	128.0	52490.306	424.130771(41)	352.6
	<i>XMM</i>	EPIC-pn/SW	0155960501	2002 Aug 06	128.4	52492.309	424.130752(40)	363.3
				Set 3 combined:	302.0	52490.306	424.130745(11)	712.7
4	<i>Chandra</i>	ACIS-S/CC ^b	3915/500394	2003 Jun 10	155.7	52800.443	424.13064(13)	26.9
	<i>Chandra</i>	ACIS-S/CC ^b	4398/500394	2003 Jun 18	115.1	52808.369	424.13084(16)	29.3
				Set 4 combined:	799.9	52800.443	424.130732(12)	53.3
5	<i>XMM</i>	EPIC-pn/SW	0304531501	2005 Jun 22	14.9	53543.515	424.1299(10)	41.7
	<i>XMM</i>	EPIC-pn/SW	0304531601	2005 Jul 05	18.0	53556.038	424.13078(92)	47.5
	<i>XMM</i>	EPIC-pn/SW	0304531701	2005 Jul 10	20.4	53561.280	424.13127(59)	58.7
	<i>XMM</i>	EPIC-pn/SW	0304531801	2005 Jul 11	63.0	53562.090	424.13088(15)	135.7
	<i>XMM</i>	EPIC-pn/SW	0304531901	2005 Jul 12	13.8	53563.283	424.13149(75)	42.2
	<i>XMM</i>	EPIC-pn/SW	0304532001	2005 Jul 17	16.5	53568.016	424.13143(66)	91.2
	<i>XMM</i>	EPIC-pn/SW	0304532101	2005 Jul 31	17.6	53582.587	424.12910(96)	32.3
			Set 5 combined:	3393.6	53543.515	424.1307512(40)	411.9	

^aPeriod derived from a Z_1^2 test. Uncertainty in last digits is in parenthesis, which is 1σ computed by the Monte Carlo method described in Gotthelf et al. (1999).

^bThese *Chandra* observations used the low-energy transmission grating (LETG).

(v3.4) and CALDB (v3.3). The photon arrival times in CC mode are adjusted in the standard processing to account for the known position of the pulsar, spacecraft dither, and SIM offset. These needed corrections were a potential cause of timing errors in earlier work, but are now accurately performed.

3. TIMING ANALYSIS

For each observation in Table 1 we transformed the photon arrival times from 1E 1207.4–5209 to Barycentric Dynamical Time (TDB) using the coordinates given in Table 2, and identified the pulsed signal using a standard FFT. To obtain a most precise value of the period in each observation we then generated a periodogram using a Z_1^2 test (Buccheri et al. 1983) around the FFT value. The 1σ uncertainty in P was determined by the Monte-Carlo method described in Gotthelf et al. (1999). In contrast to the large period changes claimed by Zavlin et al. (2004), a linear ephemeris is an excellent fit to our derived periods (see Fig. 1), with $\chi_\nu^2 = 0.65$ for 12 degrees-of-freedom, and no significant detection of a period derivative. The average period throughout the data span is $P = 424.130801(57)$ ms, with a formal 2σ upper limit of $\dot{P} < 3.9 \times 10^{-15} \text{ s s}^{-1}$.

In order to increase the precision, we refitted closely spaced observations coherently wherever possible. The results for these combined data are listed by set in Table 1, and the methods are described here. The 2005 June-July set of seven observations spanned 40 days specifically to obtain a phase-coherent timing solution. Woods et al. (2006) were not able to eliminate large phase residuals between these observations or find a unique solution. We determined that the original data processing had timing errors.

Using the reprocessed data, we iteratively measured the period and phase of adjacent observations of the 2005 data by the Z_1^2 method. Starting with the the longest observation of 2005 July 11, we extrapolated the resulting

period to the flanking observations, verifying that the predicted phase and its uncertainty matched to < 0.1 cycles the actual phase derived from the adjacent observations. After completing this procedure for all the 2005 observations a coherent fit was obtained for the entire set. Figure 2 shows the phase residuals of the individual observations from the best fit, which demonstrates the validity of the solution. The best-fit period has $Z_1^2 = 412$ and agrees with the period found above from the incoherent analysis of all observations, while the next highest peak in the power spectrum has $Z_1^2 = 275$ and is clearly an alias. To test for a \dot{P} , we then performed a Z_1^2 search on a two-dimensional grid of P and \dot{P} . The extra parameter did not increase the peak Z_1^2 significantly, meaning no detection of \dot{P} .

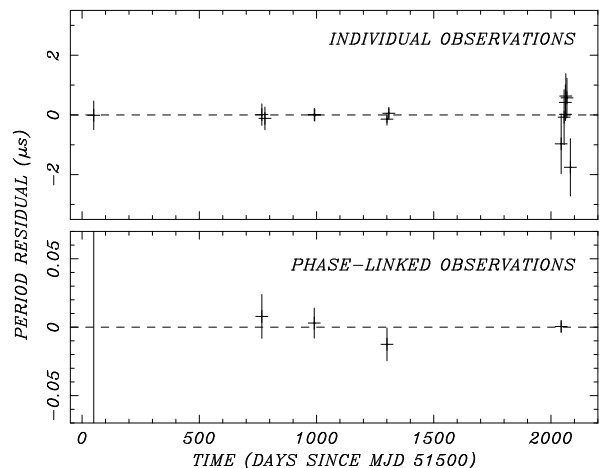


FIG. 1.— Period residuals after fitting a linear solution to individual observations (*top panel*) and grouped data sets (*bottom panel*) from Table 1. The error bar for the first individual observation is used, and continues off-scale, in the bottom panel.

The two *XMM-Newton* observations of 2002 August 4

TABLE 2
SPIN PARAMETERS OF 1E 1207.4–5209

Parameter	Value
Right ascension, R.A. (J2000) ^a	12 ^h 10 ^m 00 ^s .91
Declination, Decl. (J2000) ^a	−52°26′28″.4
Epoch (MJD)	53562
Spin period, P (s)	0.424130751(4)
Period derivative, \dot{P}	$(9.6 \pm 9.4) \times 10^{-17}$
Valid range of dates (MJD)	51549–53582
Surface dipole magnetic field, B_p (G) ^b	$< 3.5 \times 10^{11}$
Spin-down luminosity, \dot{E} (ergs s ^{−1}) ^b	$< 1.5 \times 10^{32}$
Characteristic age, τ_c (Myr) ^b	> 24

^aMeasured from *Chandra* ACIS-I ObsID 3913, in agreement with Wang et al. (2007).

^bQuantity derived from 2σ upper limit on \dot{P} .

and 6 were easily joined, resulting in the period listed in Table 1. Now knowing the precise and consistent values of P in 2002 and 2005, we were able to make a phase-connected combination of the 2001 December *XMM-Newton* observation and the 2002 January *Chandra* one, which are 13 days apart, by finding an exact period match for the correct peak from among nearby aliases. Finally, we combined the set of two *Chandra* observations spanning 2003 June 10–19, which again yielded a consistent period at the highest peak in the Z_1^2 periodogram. After making these coherent combinations, it was not possible to achieve a further phase-connected solution over a longer time span, as the intervening cycle counts could not be determined uniquely. Therefore, we made a final linear least-squares fit to the five points listed in Table 1, yielding the ephemeris presented in Table 2. This piecewise coherent measurement, yielding a 2σ upper limit of $\dot{P} < 2.8 \times 10^{-16}$, is more than an order of magnitude more precise than the fully incoherent analysis (see Fig. 1).

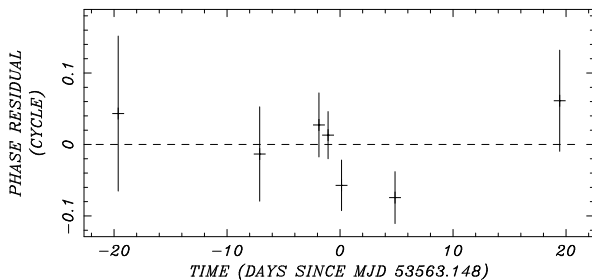


FIG. 2.— Pulse phase residuals for the 2005 *XMM-Newton* observations of 1E 1207.4–5209 after fitting a coherent timing solution using a constant period model, yielding $P = 424.1307512(40)$ ms.

4. INTERPRETATION

Contrary to previous claims, the timing behavior of 1E 1207.4–5209 does not require glitches, a binary companion, and perhaps not even accretion of fallback material, although the latter may still be needed to contribute to its X-ray spectrum and luminosity. The absence of detectable spin variations is due to a weak dipole magnetic field. In the dipole spin-down formalism, the 2σ upper limit on \dot{P} implies, for an isolated pulsar, an energy loss

rate $\dot{E} = -I\Omega\dot{\Omega} = 4\pi^2 I \dot{P} / P^3 < 1.5 \times 10^{32}$ ergs s^{−1}, surface magnetic field strength $B_p = 3.2 \times 10^{19} \sqrt{P\dot{P}} < 3.5 \times 10^{11}$ G, and characteristic age $\tau_c \equiv P/2\dot{P} > 24$ Myr. In its spin properties, 1E 1207.4–5209 is nearly a twin of another CCO, PSR J1852+0040 (Gotthelf et al. 2005; Halpern et al. 2007). The next section closely follows the discussion in Halpern et al. (2007), which anticipated the present result.

4.1. Cooling and/or Accreting

The X-ray luminosity of 1E 1207.4–5209 is of thermal origin, with $L_{\text{bol}} \approx 2 \times 10^{33} (d/2 \text{ kpc})^2$ ergs s^{−1} (De Luca et al. 2004). This is much larger than the upper limit on its spin-down power, \dot{E} , and argues that it is mostly residual cooling. However, fits to the spectrum require two blackbody components; the hotter one, of temperature $kT_{\text{BB}} = 0.32$ keV, has an area of only 0.87 km² (De Luca et al. 2004), which may indicate heating by accretion onto the polar cap. The canonical area of the open-field-line polar cap is $R_{\text{pc}} = 2\pi^2 R^3 / Pc \approx 0.27$ km². This is $\sim 30\%$ of the fitted blackbody component, but accretion may cover a wider area.

The characteristic age $\tau_c > 24$ Myr, compared to the remnant age, estimated as 7 kyr with an uncertainty of a factor of 3 (Roger et al. 1988), requires that pulsar was born spinning at its current period. A recent population analysis of radio pulsars favors a wide distribution of birth periods (Faucher-Giguère & Kaspi 2006), in which 424 ms would be typical. Furthermore, as magnetic field is generated by a turbulent dynamo whose strength depends on the rotation rate of the proto-neutron star (Thompson & Duncan 1993), it is natural that pulsars born spinning slowly would have the weaker B -fields; the model of Bonanno et al. (2006) supports this.

There are no young radio pulsars with $B_p < 10^{11}$ G. Since 1E 1207.4–5209 is not necessarily beyond the radio pulsar death line, either empirical (Faucher-Giguère & Kaspi 2006) or theoretical (Chen & Ruderman 1993), there may be another reason it is radio quiet. It is possible that low-level accretion of SN debris prevents CCOs from becoming radio pulsars for thousands or even millions of years. Accretion from a fallback disk (Alpar 2001; Shi & Xu 2003; Ekşi et al. 2005; Liu et al. 2006) was one of the theories considered by Zavlin et al. (2004) to explain the now defunct timing irregularities of 1E 1207.4–5209. But accretion may still be needed to account for its radio-quiet and X-ray-hot properties.

If the magnetic field is weak enough that an accretion disk can penetrate the light cylinder, the hotter portion of the NS surface in 1E 1207.4–5209 can be powered by accretion of only $\dot{m} \approx 10^{13}$ g s^{−1}. It is required that $B_p < 5 \times 10^{11}$ G for 1E 1207.4–5209 to be able to accrete in the propeller regime. But in this limit, the pulsar would tend to spin down at a rate that is excluded by observations,

$$\dot{P} \approx 1.2 \times 10^{-14} \mu_{29}^{8/7} \dot{M}_{13}^{3/7} \left(\frac{M}{M_{\odot}} \right)^{-2/7} I_{45}^{-1} \left(\frac{P}{0.424 \text{ s}} \right),$$

where the magnetic moment $\mu = B_p R^3 / 2 \approx 10^{29} B_{p,11}$ G cm³. Also, \dot{M} would have to be greater than 10^{13} g s^{−1}, as most of the accreting matter is expelled from the magnetospheric radius rather than accreted.

However, if $B_p < 2 \times 10^9$ G, then 1E 1207.4–5209 may accrete as a “slow rotator,” and spin up at a small rate,

$$\dot{P} \approx -2.1 \times 10^{-17} \mu_{27}^{2/7} \dot{m}_{13}^{6/7} \left(\frac{M}{M_\odot} \right)^{3/7} \left(\frac{P}{0.424 \text{ s}} \right)^2.$$

In this regime, secular spin-up, and torque noise, which may be of the same magnitude, are below the sensitivity of the existing measurements.

While flickering is also an indicator of accretion, we do not have strong evidence of variability of 1E 1207.4–5209 (< 1% on month timescales). Also, upper limits on optical/IR emission from 1E 1207.4–5209 are comparable to that expected from a geometrically thin, optically thick disk accreting at the rate required to account for its X-ray luminosity (Zavlin et al. 2004; Wang et al. 2007). Therefore, it may be necessary to invoke a radiatively inefficient flow in order to consider accretion.

4.2. X-ray Absorption Lines

Broad absorption lines in the soft X-ray spectrum of 1E 1207.4–5209 are centered at 0.7 keV and 1.4 keV (Sanwal et al. 2002; Mereghetti et al. 2002), and possibly at 2.1 keV and 2.8 keV (Bignami et al. 2003; De Luca et al. 2004), although the reality of the two higher-energy features has been disputed (Mori et al. 2005). Proposed absorption mechanisms include electron cyclotron in a weak (8×10^{10} G) magnetic field (Bignami et al. 2003; De Luca et al. 2004), atomic features from singly ionized helium in a strong (2×10^{14} G) field (Sanwal et al. 2002; Pavlov & Bezchastnov 2005), and iron (Mereghetti et al. 2002), or oxygen/neon in a normal (10^{12} G) field (Hailey & Mori 2002; Mori & Hailey 2006).

Our upper limit, $B_p < 3.5 \times 10^{11}$ G, favors the electron cyclotron model, for at least one of the lines, over all others that require stronger fields. The cyclotron prediction, 8×10^{10} G, assumes that 0.7 keV is the fundamental energy $E_c = 1.16(B/10^{11} \text{ G})/(1+z)$, where z is the gravitational redshift. Another solution postulates hydrogenic oxygen for the 0.7 keV line, while the 1.4 keV line is the cyclotron fundamental (Hailey & Mori 2002; Mori & Hailey 2006). As these authors pointed out, abundant oxygen may be accreted from supernova debris. One caveat, however, is that the magnetic field strength at the NS surface can be larger in places than the global dipole that determines the spin-down rate.

4.3. Are CCOs a Class?

The half dozen radio-quiet CCOs are similar in their X-ray luminosities, high temperatures, and absence of pulsar wind nebulae. Therefore, they may comprise a fairly uniform class defined by a weak magnetic field, which in turn results from slow natal rotation. If accreting, a slow initial spin is still unavoidable, since even at

Eddington-limited accretion rates, the spin-up and spin-down time scales in §3.1 and in Halpern et al. (2007) are much longer than the ages of the remnants. While we do not have definite evidence of accretion in any CCO, small B_p and large P both make it possible for a pulsar to accrete at low rates from a SN debris disk; the large B_p and rapid spin of young radio pulsars prevents such a disk from penetrating the light cylinder. In order to test the general applicability of these results to the class of CCOs, more sensitive searches for their pulsations are required. However, prior null results on all of them suggest that their pulsed amplitudes are very small.

5. CONCLUSIONS

A comprehensive analysis of all timing data on the X-ray pulsar 1E 1207.4–5209 has resolved the dilemma of its mysterious spin properties by correcting previous errors in data processing and analysis. It is simply a low magnetic field NS that has no discernible variation in spin over 5 years. If an isolated NS, the upper limit on its spin-down power is much less than its bolometric X-ray luminosity, which leaves only internal cooling and/or accretion as possible energy sources. In either case, 1E 1207.4–5209 must have been born with a weak magnetic field and its long rotation period. We speculate that these two parameters are causally related and, projecting from the near twins 1E 1207.4–5209 and PSR J1852+0040, possibly the physical basis of the CCO class.

An additional benefit of this solution is the new constraint on proposed absorption-line models for 1E 1207.4–5209 that depend on the magnetic field strength. Our upper limit on the dipole field is close to the prediction of the electron cyclotron model for both lines, and perhaps oxygen for one of the lines. To actually make a significant measurement of B_p as small as 8×10^{10} G from dipole spin-down would require a fully phase-coherent timing solution spanning $\gtrsim 6$ yr, assuming that there is no glitch or other timing noise. Such a program would also be sensitive to accretion torques at the lowest rates predicted here for spin-up. In case B_p is as small as 10^9 G and some of the X-ray luminosity of 1E 1207.4–5209 is due to accretion from a debris disk, spin-up could be detected.

This investigation is based on observations obtained with *XMM-Newton*, an ESA science mission with instruments and contributions directly funded by ESA Member States and NASA. Support for this work was provided by NASA through *XMM* grant NNX06AH95G and *Chandra* Award SAO GO6-7048X.

REFERENCES

- Alpar, M. A. 2001, *ApJ*, 554, 1245
 Bignami, G. F., Caraveo, P. A., De Luca, A., & Mereghetti, S. 2003, *Nature*, 423, 725
 Bonanno, A., Urpin, V., & Belvedere, G. 2006, *A&A*, 451, 1049
 Buccheri, R., et al. 1983, *A&A*, 128, 245
 Chen, K., & Ruderman, M. 1993, *ApJ*, 402, 264
 De Luca, A., Mereghetti, S., Caraveo, P. A., Moroni, M., Mignani, R. P., & Bignami, G. F. 2004, *A&A*, 418, 625
 Ekşi, K. Y., Hernquist, L., & Narayan, R. 2005, *ApJ*, 623, L41
 Faucher-Giguère, C.-A., & Kaspi, V. M. 2006, *ApJ*, 643, 332
 Gotthelf, E. V., Halpern, J. P., & Seward, F. D. 2005, *ApJ*, 627, 390
 Gotthelf, E. V., Vasisht, G., Dotani, T. 1999, *ApJ*, 522, L49
 Hailey, C. J., & Mori, K. 2002, *ApJ*, 578, L133
 Halpern, J. P., Gotthelf, E. V., Camilo, F., & Seward, F. D. 2007, *ApJ*, submitted
 Helfand, D. J., & Becker, R. H. 1984, *Nature*, 307, 215
 Kirsch, M. G. F., et al. 2004, *SPIE*, 5165, 85
 Liu, D. B., Yuan, A. F., Chen, L., & You, J. H. 2006, *ApJ*, 644, 439

- Mereghetti, S., De Luca, A., Caraveo, P. A., Becker, W., Mignani, R., & Bignami, G. F. 2002, *ApJ*, 581, 1290
- Mori, K., Chonko, J. C., & Hailey, C. J. 2005, *ApJ*, 631, 1082
- Mori, K., & Hailey, C. J. 2006, *ApJ*, 648, 1139
- Pavlov, G. G., & Bezchastnov, V. G. 2005, *ApJ*, 635, L61
- Pavlov, G. G., Sanwal, D., & Teter, M. A. 2004, in *IAU Symp 218, Young Neutron Stars and their Environments*, ed. F. Camilo & B. M. Gaensler (San Francisco: ASP), 239
- Pavlov, G. G., Zavlin, V. E., Sanwal, D., & Trümper, J. 2002, *ApJ*, 569, L95
- Roger, R. S., Milne, D. K., Kesteven, M. J., Wellington, K. J., & Haynes, R. F. 1988, *ApJ*, 332, 940
- Sanwal, D., Pavlov, G. G., Zavlin, V. E., & Teter, M. A. 2002, *ApJ*, 574, 61
- Shi, Y. & Xu, R. X. 2003, *ApJ*, 596, L75
- Thompson, C., & Duncan, R. C. 1993, *ApJ*, 408, 194
- Wang, Z., Kaplan, D. L., & Chakrabarty, D. 2007, *ApJ*, 655, 261
- Woods, P. M., Zavlin, V. E., & Pavlov, G. G. 2006, in *Proc. Isolated Neutron Stars: from the Interior to the Surface*, ed. D. Page, R. Turolla, & S. Zane, in press (astro-ph/0608483)
- Zavlin, V. E., Pavlov, G. G., & Sanwal, D. 2004, *ApJ*, 606, 444
- Zavlin, V. E., Pavlov, G. G., Sanwal, D., & Trümper, J. 2000, *ApJ*, 540, L25